1   **A high fat/cholesterol diet recapitulates some Alzheimer's disease-like**

2   **features in mice: focus on hippocampal mitochondrial dysfunction**

3

4   Gianni **Mancini**[a], Candida **Dias**[b,c], Catia F. **Lourenço**[b,c], Joao **Laranjinha**[b,c], Andreza **de**

5   **Bem**[a,d,†], Ana **Ledo**[b,c, ‡]

6

7   [a] Departamento de Bioquímica, Universidade Federal de Santa Catarina, Florianópolis,

8   Brazil

9   [b] Center for Neuroscience and Cell Biology, University of Coimbra, Coimbra, Portugal

10   [c] Faculty of Pharmacy, University of Coimbra, Coimbra, Portugal

11   [d] Department of Physiological Sciences, Institute of Biological Sciences, University of Brasília,

12   Brasília, Brazil.

13

14   [*] **Corresponding Authors:**

15   [‡] Ana **Ledo**

16   analedo@ff.uc.pt

17   Faculty of Pharmacy, University of Coimbra

18   Health Science Campus

19   Azinhaga de Santa Comba

20   3000-548 Coimbra, Portugal

21

22   [†]Andreza Fabro **de Bem**

23   debemandreza@gmail.com

24   Department of Physiological Sciences

25   Institute of Biological Sciences

26   University of Brasília

27   Brasília, Brazil

Abstract

Background: Ample evidence from clinical and pre-clinical studies suggests mid-life hypercholesterolemia as a risk factor for developing Alzheimer's disease (AD) at a later age. Hypercholesterolemia induced by dietary habits can lead to vascular perturbations that increase the risk of developing sporadic AD. **Objective**: To investigate the effects of a high fat/cholesterol diet (HFCD) as a risk factor for AD by using a rodent model of AD and its correspondent control (healthy animals). **Methods:** We compared the effect of a HFCD in normal mice (non-transgenic mice, NTg) and the triple transgenic mouse model of AD (3xTgAD). We evaluating cognitive performance in relation to changes in oxidative metabolism and neuron-derived nitric oxide ($^\bullet$NO) concentration dynamics in hippocampal slices as well as histochemical staining of markers of the neurovascular unit. **Results:** In NTg the HFCD produced only moderate hypercholesterolemia but significant decline in spatial memory was observed. A tendency for decrease in $^\bullet$NO production was accompanied by compromised mitochondrial function with decrease in spare respiratory capacity. In 3xTgAD mice, a robust increase in plasma cholesterol levels with the HFCD did not worsen cognitive performance but did induce compromise of mitochondrial function and significantly decreased $^\bullet$NO production. We found increased staining of biomarkers for astrocyte endfeet and endothelial cells in 3xTgAD hippocampi, which was further increased by the HFCD. **Conclusion:** A short term (8 weeks) intervention with HFCD can produce an AD-like phenotype even in the absence of overt systemic hypercholesterolemia and highlight mitochondrial dysfunction as a link between hypercholesterolemia and sporadic AD.

Keywords: Alzheimer's disease; high fat/cholesterol diet; hippocampus; spare respiratory capacity.

Introduction

Alzheimer's disease (AD) is a multifactorial neurodegenerative disease attributable to several interrelated and interacting environmental and genetic factors [1]. Sporadic AD, in which the major risk factor is aging, accounts for up to 95% of all cases. Evidence from both clinical and pre-clinical studies indicate that life-style associated vascular risk factors including, obesity [2], hypercholesterolemia [3], hypertension [4], atherosclerosis [5], and diabetes [6] play a critical role in development of AD. Changes in cholesterol homeostasis and consequent increases in plasma cholesterol levels have been implicated in AD pathogenesis [5,7] and clinical studies have shown that individuals with high serum cholesterol levels in midlife are more susceptible to develop AD later in life [3]. Furthermore, the *ε4* allele of apolipoprotein E (Apo E) has consistently been demonstrated to be a genetic risk factor for sporadic AD, supporting a role for cholesterol in the pathogenesis of AD [7–9].

Chronic exposure to high serum cholesterol levels causes functional impairment of the vascular endothelium leading to cerebrovascular dysfunction and blood-brain barrier (BBB) breakdown [10]. The vascular hypothesis of AD rationalizes the causal relationship between the vascular impairments and development of sporadic AD, proposing that long-lasting cerebrovascular dysfunction results in brain hypoperfusion with consequent neuronal energy crisis and inadequate clearance at the BBB, namely of ß-amyloid [11]. A cascade of subsequent downstream events may lead to metabolic changes, neuroinflammation, ß-amyloid accumulation and tau pathology, ultimately contributing to the onset of AD [12].

On the other hand, decline in energy metabolism is a critical feature of the aging brain. The hypometabolic state observed in neurodegenerative disorders such as AD results from decreased supply in substrates, mitochondrial dysfunction and impaired energy transduction [13,14]. Growing evidence suggests that mitochondrial dysfunction precedes plaque and neurofibrillary tangle formation [15] and oxidative damage resulting from mitochondrial dysfunction has been observed in patients suffering of mild cognitive impairment (MCI), suggesting that it may be an early event in AD pathogenesis [16,17]. Clinical studies have also

82   revealed decreased glucose uptake both in MCI and AD patients [18–20], further

83   substantiating energetic crisis as an early event in AD.

84   One putative central element which may crosslink mitochondrial, synaptic and vascular

85   dysfunction as well as neuro-inflammation in AD is nitric oxide ($^{\bullet}$NO) [21]. Nitric oxide is known

86   to play a role in synaptic activity, neural plasticity and memory functions in particular in the

87   hippocampus [22] where NMDAr activation leads to transient production of $^{\bullet}$NO [23] that, in

88   turn, may ultimately lead to changes in synaptic plasticity as a result of increased cGMP levels

89   (due to activation of soluble guanylate cyclase (sGC) [24] and *S*-nitrosylation of key proteins

90   (including several ion channels) [25]. Finally, $^{\bullet}$NO may play a critical role as a master-regulator

91   of brain energy metabolism via reversible inhibition of oxidative phosphorylation at cytochrome

92   *c* oxidase, upregulation of astrocytic glycolysis, regulation of glucose transport to neurons and

93   astrocytes and regulating the fate of glucose in neurons (reviewed in [26,27]).

94   In the present work, we investigate the effects of a high fat/cholesterol diet (HFCD) as a

95   risk factor for AD by using a rodent model of AD versus its correspondent control (healthy

96   animals). We compared cognitive status, oxidative phosphorylation and $^{\bullet}$NO concentration

97   dynamics between non-transgenic (NTg) mice fed an 8-week HFCD and age-matched triple

98   transgenic AD mice (3xTgAD). We focused on the hippocampus, a structure of the CNS that

99   is prominently compromised in AD [28]. Our results show that although HFCD did not intensify

100   the already installed cognitive impairment in 3xTgAD mice, it induced an impairment of

101   hippocampal spatial short-term memory in NTg mice which was accompanied by decrease in

102   the maximal $^{\bullet}$NO concentration and mitochondrial O_2 consumption in hippocampal slices.

Materials and Methods

Animals and Experimental Design

The present study was performed using the triple transgenic mouse model of Alzheimer's disease (3xTgAD) harboring AD-related human mutations (APP$_{swe}$, PS1$_{M146V}$, and Tau$_{P301L}$ transgenes) [29] and age-matched non-transgenic (NTg) mice (129SV x C57BL/6). Both male (4/5 per group) and female (3/4 per group) mice aged 3 to 4 mo., were supplied from a colony implemented in the animal facility of the Center for Neuroscience and Cell Biology (Coimbra) obtained from Frank M. LaFerla's Laboratory at the department of Neurobiology and Behavior, Institute for Brain Aging and Dementia (University of California, Irvine, USA). Animals were maintained in a 12/12-h light/dark cycle, at 21±2 °C. They were allowed free access to tap water and food. All experiments were performed in accordance with the European Community Council Directive for the Care and Use of Laboratory Animals and approved by the Animal Care Committee of the Center for Neuroscience and Cell Biology of Coimbra (Ref. ORBEA_92_2014/10042014).

Animals were separated into 4 groups (n=8/9 per group): two (NTg and 3xTgAD) receiving control diet (regular chow, CD groups) and another two (NTg and 3xTgAD) receiving a high fat/cholesterol diet (HFCD groups) for a period of 67 days. The HFCD (Research Diets, D14022601) was composed of 1.25% cholesterol, 20% fat and 0.5% cholic acid. Table SI (Supplementary Material) shows the comparative composition of the HFCD and CD. Body weight was monitored weekly for the full course of treatment. At the end of the 60-day treatment period all animals were subject to behavioral testing spanning a 7-day period. Following this, 4/5 animals in each group were randomly selected for biochemical and electrochemical analysis, while 4 were used for immunohistochemical analysis. In the first instance, animals were euthanized by decapitation. Brains were quickly removed and hippocampi were dissected slice preparation. Blood was collected from these animals upon decapitation. Animals used for immunohistochemical analysis were perfused transcardially

130   and brain was dissected and preserved analysis. The experimental design of the present study

131   is depicted in Fig. 1A.

132

133   **Plasma Cholesterol Levels**

134   Blood was collected after an overnight fasting period and before euthanasia and was

135   centrifuged (3500g, 10 min) to isolate the plasma. Plasma cholesterol levels were measured

136   using an enzymatic kit and according to the manufacturer's instructions (Labtest Diagnóstica

137   SA, Minas Gerais, Brazil).

138

139   **Behavioral Tests**

140   All tests were carried out between 10:00 AM and 5:00 PM in a sound-attenuated room

141   under low-intensity light (12 lx). Mice were allowed a 1h habituation period in the room before

142   the beginning of the tests. Animal behavior was monitored through a video camera positioned

143   above the apparatuses and videos were later analyzed using the ANY Maze video tracking

144   system (Stoelting Co., Wood Dale, IL, USA).

145   *Open Field Activity:* Mice were placed into the center of the square arena of the open field

146   apparatus (50x50x40 cm) made of grey PVC for 10 min on two consecutive days. The distance

147   travelled (cm) was collected in 2-min intervals.

148   *Novel object recognition task:* The novel object recognition test was carried out 24 h after

149   the test session (second day) in the same apparatus used for open field activity on previous

150   day [30]. The task consisted of two 5-min sessions (training and test) separated by a 90-min

151   interval. In the training session, two identical objects were placed near the two opposing

152   corners of the arena and in the test session one of the objects was replaced with a novel

153   object. In each session, mice were allowed to explore the objects for 5 min. We considered to

154   score object exploration whenever the mouse sniffed the object or touched the object while

155   looking at it (i.e., when the distance between the nose and the object was less than 2 cm).

156   The discrimination ratio was defined as the ratio between the time spent exploring the novel

157   object (T_N) and the total time spent exploring both the novel and familiar object (T_N+T_F): $T_N/(T_N$

158    $+ T_F$).

159   ***Modified Y-Maze:*** The modified Y-maze task was used to assess short-term spatial memory

160   and is based on the innate preference of animals to explore novel areas [31]. The Y-maze

161   apparatus consisted of three arms (18 x 6 x 6 cm) made of wood covered with impermeable

162   Formica. This task consisted of two 8-min trials (training and test) separated by an inter-trial

163   interval of 90 min. During the training trial, one arm ("novel") was left blocked by a removable

164   door. During the test trial, the "novel" arm was opened. The percentages of entries and time

165   spent in each arm were recorded.

166

167   **Preparation of Mouse Hippocampal Slices**

168   For the study of hippocampal $^{\bullet}NO$ concentration dynamics and tissue oxygen

169   consumption rates, the hippocampi of mice from all 4 groups were rapidly dissected from brain

170   following decapitation and placed on the stage of a McIlwain tissue chopper (Campden

171   Instruments, London, UK), 250-µm-thick sections were obtained for to oxygen consumption

172   and 400-µm-thick sections were obtained for to electrophysiology and $^{\bullet}NO$ concentration

173   dynamics. The slices were separated and transferred to a pre-incubation chamber (BSC-PC;

174   Harvard Apparatus) filled with artificial cerebrospinal fluid (aCSF) containing (in mM); 124

175   NaCl, 4.5 KCl, 2 $CaCl_2$, 1 $MgCl_2$, 26 $NaHCO_3$, 1.2 NaH_2PO_4 and 10 D-glucose, gassed with a

176   gas mixture of 95% O_2 and 5% CO_2 (carbox) at room temperature. Slices were allowed to

177   recover under these conditions for at least 1 h prior to recording.

178

179   **Nitric Oxide Concentration Dynamics**

180   Carbon fiber microelectrodes (CFM) used to record nitric oxide concentration dynamics

181   in hippocampal slices were fabricated as previously described [32]. Briefly, a single carbon

182   fiber (30 µm o.d.; Textron Lowell, MA, USA) was inserted into a borosilicate glass capillary

183   (1.16 mm i.d. and 2.0 mm o.d.; Harvard Apparatus, Holliston, MA, USA). Each capillary was

184   pulled on a vertical puller (Harvard Apparatus, UK) and the protruding carbon fiber was cut to

185   a tip length of approx. 150 μm. The electrical contact between the carbon fiber and the copper

186   wire was provided by conductive silver paint (RS, Northants, UK). The microelectrodes were

187   tested for general recording properties in 0.05 M PBS Lite (in mM: 10 Na_2HPO_4, 40 NaH_2PO_4,

188   and 100 NaCl, pH 7.4) by fast cyclic voltammetry at a scan rate of 200 V s^{-1}, between -1.0 and

189   +1.0 V vs. Ag/AgCl for 30 s (Ensman Instruments, USA). To improve electroanalytical

190   performance, each CFM was coated with 2 layers of Nafion® and electropolymerized *o*-

191   phenylenediamine (*o*-PD). A 5 mM o-PD solution in PBS Lite was made fresh each day and

192   used immediately. Electropolymerization was performed by amperometry at +0.7 V vs.

193   Ag/AgCl, for 3 periods of 15 min using a CompactStat Potentiostat (IVIUM Technologies BV,

194   The Netherlands).

195   Each CFM for ˙NO was evaluated in terms of sensitivity for ˙NO (using a saturated ˙NO

196   solution prepared as described in [33]) and selectivity against the major interfering analytes in

197   the brain (ascorbate and nitrite). Individual slices were placed in a recording chamber (BSC-

198   BU with BSC-ZT top; Harvard Apparatus) and perfused at a flow rate of 2 mL/min with aCSF

199   at 32°C (temperature controller Model TC-202A; Harvard Apparatus) continuously bubbled

200   with humidified carbox. The CFM was inserted into the pyramidal cell layer of the CA1

201   subregion of the rat hippocampal slice, 100–200 μm into the tissue. Amperometric recording

202   of ˙NO was performed by amperometry at +0.9V vs. Ag/AgCl using the CompactStat

203   Potentiostat in a 2-electrode configuration. Once a stable background current was obtained,

204   endogenous ˙NO production was evoked with NMDA (100 μM) added to the perfusion medium

205   for 2 min. The ˙NO signals were characterized in terms of peak amplitude of the ˙NO signal,

206   converted into concentration using the calibration ($[˙NO]_{max}$) and half-width of the signal.

207

208   **Oxygen Consumption Rate in Whole Hippocampal Slices**

209   Oxygen consumption rate in intact hippocampal slices was measured by high-resolution

210   respirometry (Oxygraph-2k, OROBOROS Instruments, Innsbruck, Austria) at 32ºC as

211   described in [34]. Air calibration was carried out before every experiment and in accordance

212   with equipment instructions. Data acquisition and analysis was performed using DatLab

213 software 5.0 (OROBOROS Instruments, Innsbruck, Austria). The hippocampal slices were

214 place in a holder consisting of a nylon mesh glued to a polypropylene ring (o.d. 1.6 cm) fitting

215 tightly in the recording chamber. Measurements were carried out with continuous stirring,

216 using 2 mL of aCSF containing 20 mM HEPES and 10 mM pyruvate. Due to the high O_2

217 requirement of hippocampal slices, experiments were performed at high $[O_2]$ and chambers

218 were re-oxygenated throughout the experiment. After stabilization of tissue respiration, drugs

219 were injected in the following order: carboxyatractyloside (12.5 µM) and oligomycin (20

220 µg/mL), FCCP (20 µM, titration), rotenone (2.2 µM), and antimycin A (12.5 µM).

221 Prior to measurements and in order to allow correction of raw oxygen consumption rate

222 by wet tissue weight, slices were weighed in a high precision scale. Slices were transferred

223 into the holder which was then carefully dried in tissue paper. An average of 5 mg of tissue

224 was used in each experiment [35].

225

226 **Immunohistochemistry**

227 Mice were deeply anesthetized and were perfused through the left cardiac ventricle with

228 ice-cold 0.9% saline solution, followed by ice-cold 4% paraformaldehyde in 0.1M PBS (pH

229 7.4). After perfusion, brains were removed, post-fixed in the same fixative solution for 24h at

230 4ºC, and cryoprotected by immersion in a 30% sucrose solution in PBS at 4ºC. The brains

231 were then frozen by immersion in cooled isopentane and stored at −80ºC for later analyses.

232 Serial coronal sections (40 µm) containing the hippocampus were obtained with a cryostat

233 (Leica) at −20ºC. The free-floating sections were first blocked using 5% horse serum (HS)

234 diluted in PBS containing 2% Triton X-100 (PBS-Tx) for 2 h at room temperature. Next the

235 sections were incubated overnight at 4ºC with anti-aquaporin 4 (Santa Cruz Biotechnology,

236 AQP4, 1:100, sc-9888) from goat in 1% HS diluted in 0.5% PBS-Tx. After three washes in

237 PBS, tissue sections were incubated with anti-goat Alexa 568 (Invitrogen, 1:400, A11079) in

238 1% HS diluted in 0.5% PBS-Tx for 2 h at room temperature. For tomato lectin immunostaining,

239 the free-floating sections were first permeabilized in tris-buffered saline (TBS) containing 1%

240 Triton X-100 for 2 h at room temperature. Next the sections were incubated overnight at 4ºC

9

241 with *Lycopersicon esculentum* lectin (tomato lectin; Vector Laboratories, Burlingame, VT),

242 diluted 1:200. After three washes in TBS, tissue sections were incubated with Streptavidin,

243 Alexa Fluor® 568 conjugate (Santa Cruz Biotechnology, 1:500, s11226) for 2 h at room

244 temperature. Hereafter, the sections were washed three times in PBS and mounted on slides

245 with Fluor Save (Millipore, 345789), and covered with coverslips. Images from mouse

246 hippocampi were obtained with a confocal Olympus FV-10i microscope and examined and

247 quantified with Fiji ImageJ software.

248

249 **Data Analysis**

250 All the data were tested for normality by the Kolmogorov-Smirnov normality test and

251 were expressed as the mean ± SEM. Unless otherwise mentioned, statistical evaluation was

252 carried out using the two-way analysis of variance (ANOVA) with genotype and treatment as

253 independent variables. Following significant ANOVAs, multiple comparisons were performed

254 using the Bonferroni post hoc test. The novel object recognition task was analyzed by one

255 sample t-tests to determine whether the recognition index was different from 50% (random

256 investigation) and modified Y-Maze was analyzed by one sample t-tests to determine whether

257 the percentage of arm entries and percentage of time spent in each arm was different from

258 33% (random entries and time respectively). The accepted level of significance for the tests

259 was $P<0.05$. All tests were performed using GraphPad Prism 5.0 software package.

260

261

Results

Body Weight and Plasma Cholesterol Levels

The body weight of all animals was recorded weekly during the extent of the experimental period (Fig.1B). Despite the different fat content in the two chows used, weight-gain was similar for all animal groups: 17.6 ± 2.5 % and 17.6 ± 3.6% for the NTg and 3xTgAD groups fed CD, respectively; 15.7 ± 8.2% and 17.9 ± 5.7% for NTg and 3xTgAD fed HFDC, respectively.

On the final day of the 8-week experimental period, blood was collected from all animals and plasma was separated for quantification of plasma cholesterol levels. As observed in Fig. 1C, NTg and 3xTgAD on CD had similar plasma cholesterol levels (55.5 ± 1.0 mg dL^{-1}, N=8 and 53.41 ± 1.39 mg dL^{-1}, N=8, respectively). In NTg mice, the HFCD produced a tendency (10%) for increase in plasma cholesterol levels (61.7 ± 1.6 mg dL^{-1}, N=5), while a significant increase was observed for 3xTgAD (76.01 ± 3.36 mg dL^{-1}, N=7). The observed differences were due to both diet ($F_{(1,24)} = 48.71$, P<0.0001) and genotype ($F_{(1,24)} = 8.75$, P=0.0069), with a significant interaction between the two factors ($F_{(1,24)} = 15.91$, P=0.0005).

Locomotor Activity and Cognitive Performance

Locomotor activity was evaluated in an open field arena and the total distance travelled during the 10-minute period of the test was determined. As shown in Fig. 2A (and in Supplemental Material - Figure S1A), the 3xTgAD-CD mice showed a tendency for decrease in locomotor activity as compared to NTg-CD mice (465.35 ± 114.77 cm, N=4 and 774.50 ± 136.86 cm, N=6, respectively). The HFCD induced a small increase in locomotor activity in the NTg mice (843.17 ± 165.41 cm, N=8) and a significant increase in the 3xTgAD mice (988.01 ± 91.93 cm, N=9) as compared to the 3xTgAD-CD group. A significant effect was observed for diet ($F_{(1,23)} = 4.3$, P=0.0049), but not for genotype ($F_{(1,23)} = 0.33$, P=0.571).

Analysis of the partial distances for each 2-min block of the 10-min test (Fig. 2B) revealed that the NTg-CD group (grey triangles) displayed an expected decrease in locomotor activity throughout the test, while the NTg-HFCD group (green triangles) retained a higher

11

290   index of locomotor activity. This was also evident for the 3xTgAD-HFCD group (green squares)

291   relative to the 3xTgAD-CD group (grey squares). In other words, the increased total distance

292   observed in the HFCD-fed groups relative to the CD fed groups appears to result from a lack

293   of habituation.

294   Spatial memory was evaluated using a modified Y-maze task. As shown in Fig. 2C and

295   D, the percentage of entries into and relative time spent in the "novel" arm was significantly

296   above chance performance (33.3%, P<0.05, one-sample t-test analysis) only for the NTg-CD

297   group (44.7 ± 1.0 %, N=7 and 60.2 ± 2.9 %, N=8, respectively). The 3xTgAD-CD group showed

298   compromised learning performance, as expected at this age, expressed as a decrease in

299   percentage of entries into the novel arm and a significant decrease in the time spent in the

300   novel arm. We further observed that the NTg-HFCD group showed a similar compromise in

301   learning as the 3xTgAD-CD mice – neither percentage of entries nor time spent in the novel

302   arm were found to be statistically different from chance performance. The 3xTgAD-HFCD

303   showed equally compromised learning performance in the y-maze test.

304   Both genotype ($F_{(1,28)}$=23.34, P<0.0001) and diet ($F_{(1,28)}$=11.06, P=0.0025) had a

305   significant effect over the results for time spent in the novel arm, and the interaction between

306   the 2 factors was also significant ($F_{(1,28)}$=5.756, P=0.0233). In the training trial, statistical

307   analysis showed a similar number of entries and percentage of time in the arms for all groups

308   (see Supplemental Figure S2, C - D).

309   The novel object recognition task corroborated the results obtained in the y-maze, as

310   only the NTg-CD group demonstrated a recognition index significantly above chance

311   performance (50%) (Fig. 2E; P<0.05, one-sample t-test analysis). The recognition index was

312   significantly decreased for the 3xTgAD-CD and NTg-HFCD groups as compared to the control

313   NTg-CD mice. Neither diet nor genotype had a significant effect on variance, although a

314   significant interaction between the 2 factors was determined ($F_{(1,24)}$ = 5.677, P=0.0255).

315   Taken together, this behavioral analysis firstly confirms the expected AD-like cognitive

316   impairment expected at 6 mo. of age in the 3xTgAD mouse model [36,37]. From this we

317   hypothesize that a HFCD induces biochemical and cellular alterations in the CNS of mice

318   which leads to the expression of a behavioral phenotype similar to that observed in the AD

319   model. As the cognitive impairment is already installed at this age, the HFCD cannot further

320   aggravate it in the 3xTgAD mice.

321

322   **Nitric Oxide Concentration Dynamics Linked to Glutamate Receptor Activation**

323   Considering that ·NO acts as a retrograde messenger in NMDA-dependent synaptic

324   events in the hippocampus [22], we investigated the effect of the HFCD on NMDAr-evoked

325   ·NO concentration dynamics in the CA1 *st. pyramidale* layer. We found that transient activation

326   of NMDA receptors (2 min perfusion, 100 µM) induced a transient increase in ·NO

327   concentration measured in the CA1 subregion of hippocampal slices from all groups, as

328   expected [13]. Quantification of peak [·NO] is shown in Fig. 3A. As we previously reported, a

329   significant increase in peak [·NO] in 3xTgAD-CD mice (2.07 ± 0.42 µM, N=35) was observed

330   when comparing to NTg-CD mice (0.56 ± 0.09, N=30). However, the HFCD induced a

331   tendency for decreased [·NO]$_{max}$ in NTg group (0.345 ± 0.07 µM, N= 11) and a significant

332   decrease in the 3xTgAD group (0.29 ± 0.08 µM, N=15). Genotype ($F_{(1,87)}$=4.103, P= 0.0459)

333   and diet ($F_{(1,87)}$=6.849, P= 0.0105), as well as the interaction between the two factors

334   ($F_{(1,87)}$=4.170, P= 0.0442), were shown to have a significant effect over the observed

335   differences. Furthermore, the HFCD induced a tendency for increase of the ½ width of the

336   signals (Fig. 3B) in both NTg and 3xTgAD groups, indicating slower ·NO production and

337   removal kinetics. We found no significant difference in production and decay rates (not

338   shown).

339

340   **Mitochondrial oxidative phosphorylation in intact hippocampal tissue**

341   Adequate mitochondrial function and energy supply are key in supporting synaptic

342   function. As such, mitochondrial dysfunction and bioenergetic crisis have been suggested to

343   be key elements of the pathophysiology of AD. We assessed the effects of HFCD treatment

344   on mitochondrial respiration using high-resolution respirometry (HRR) to evaluate the O_2

345   consumption rates (OCR) in intact hippocampal slices. Figure 4A shows a representative

oxygraphy trace of a full substrate-uncoupler-inhibitor titration (SUIT) protocol using intact

hippocampal slices. This protocol allowed us to determine basal OCR (supported by glucose

and pyruvate); LEAK (determined following addition of oligomycin and carboxyatractyloside to

block ATP production); maximal OCR (obtained by uncoupling the mitochondrial respiratory

chain with the ionophore FCCP) as well as residual OCR resulting from non-mitochondrial O_2

consumption (obtained by blocking complexed I and III with rotenone and antimycin A,

respectively).

As shown in Fig. 4B, the AD genotype had little impact over the OCR values, except for

basal OCR which was increased in the 3xTgAD-CD when compared to the NTg-CD group.

On the other hand, the HFCD had a significant impact over tissue OCR in both NTg and

3xTgAD mice, decreasing basal, LEAK, and maximal or ETS OCR. Most relevantly, the

mitochondrial spare respiratory capacity, which is the capacity of mitochondria to increase

electron flow in situations of increased energy demand, was significantly decreased in the

NTg-HFCD as compared to the NTg-CD group and a close to significant decrease (P=0.0524)

was also observed in the 3xTgAD mice. Diet had a significant effect over observed differences

for all OCR parameters evaluated ($F_{(1,28)}$=44.94, P<0.0001 for Basal; $F_{(1,28)}$=50.56, P<0.0001

for Leak; $F_{(1,26)}$=26.97, P<0.0001 for ETS and $F_{(1,25)}$=12.04, P=0.0019 for Spare Capacity)

while the genotype had an effect for Basal ($F_{(1,28)}$=7.437, P=0.0109) and ETS ($F_{(1,26)}$=5.955,

P=0.0218).

These results suggest that, while increased intracellular amyloid load has little impact

on mitochondrial function at this age, increased cholesterol/fat resulting from an 8-week diet

change can significantly compromise mitochondrial function in the hippocampus.

Cellular components of the neurovascular unit in hippocampal slices

It has been suggested that increased cholesterol levels may compromise the

components of NVU, resulting in BBB breakdown. Immunofluorescent detection of AQP-4

(water channel primarily expressed in astrocytic foot processes) and tomato lectin (marker

used to label blood vessels and microglia) were used as surrogate biomarkers of cellular

14

374   components of NVU in the hippocampus. As can be appreciated in the series of micrographs

375   presented in Fig. 5A-D, AQP-4 immunoreactivity was increased in the CA1 subregion of the

376   3xTgAD groups. Quantification of the intensity of immunofluorescence (Fig. 5E). Subsequent

377   statistical analysis revealed that both diet and genotype had a significant effect over AQP-4

378   expression ($F_{(1,12)}$=7.932, P=0.0156 and $F_{(1,12)}$= 33.95, P<0.0001, respectively) and post hoc

379   analysis revealed a significant increase in AQP-4 fluorescence in the 3xTgAD groups as

380   compared to the diet-matched NTg groups. Also, the increase in AQP-4 immunofluorescent

381   intensity was close to significant (P=0.052) in the 3xTgAD-HFCD group as compared to the

382   3xTgAD-CD group. Similar patterns were observed in the CA3 subregion of the hippocampus

383   (Supplementary Fig. S3).

384   　　　　In line with these observations, the micrographs shown in Fig. 5F-I and the quantification

385   of immunofluorescence for tomato lectin immunoreactivity (Fig. 5J) also showed an increase

386   in the 3xTgAD groups relative to the diet-matched Ntg groups. Both genotype ($F_{(1,12)}$=17.11,

387   P=0.0014) and diet ($F_{(1,12)}$=6.153, P=0.0289) had a main effect of observed tomato lectin

388   immunofluorescence intensity. Post-hoc analysis revealed a significant increase in tomato

389   lectin immunoreactivity in the 3xTgAD-CD as compared to the NTg-CD group as well as in the

390   3TgAD-HFCD group as compares to the NTg-HFDC group.

Discussion

391

392   The origin of AD is multifactorial and many metabolic disorders originating from

393 overconsumption of high fat and cholesterol food are associated with higher risk of AD later in

394 life. Cohort studies have reported that a high plasma cholesterol level, especially when

395 measured at midlife, is associated with a poor cognitive outcome: cognitive decline, dementia,

396 and AD [38]. In animals, intake of a Western style diet, high in saturated fat and cholesterol,

397 has been shown to cause impairments in hippocampal-dependent learning and memory

398 [39,40].

399   In the present study, we hypothesized that the consumption of a HFCD may recapitulate

400 the early AD-like pathophysiological features observed in the triple transgenic mouse model

401 for AD. We found that NTg mice receiving the HFCD expressed behavioral alterations similar

402 to cognitive changes observed in 3xTgAD mice. Despite the modest increase in plasma

403 cholesterol levels (ca. 10%), HFCD was associated with spatial memory deficits in modified

404 Y-maze and novel object recognition task in NTg mice. Furthermore, the HFCD induced a

405 hyperactive phenotype and failure to habituate to open field apparatus in NTg mice, which is

406 in good agreement with previous reports showing that hypercholesterolemic LDLr$^{-/-}$ mice

407 exhibited increased locomotor activity assessed in the open field test [41]. These results

408 suggest that the effects of HFCD may be due to lack of spatial habituation which is a function

409 of hippocampal-dependent short-term spatial memory [42]. Although the BBB prevents lipid

410 exchange between the periphery and the CNS, several studies have shown that increased

411 dietary cholesterol intake may impact cognition and produce an AD-like phenotype. In

412 particular, HFCD fed Swiss mice, hypercholesterolemic LDLr$^{-/-}$ mice [40,43] and rats fed a high

413 cholesterol diet [44] have been shown to exhibit hippocampal-dependent learning and memory

414 impairments. Other studies have also shown that a 5-month high cholesterol diet (5%) slightly

415 impacts memory performance in wild type mice [45] while a 3-month high fat diet produced no

416 change in cognitive performance in WT mice [46]. Interestingly, a HFCD does not necessarily

417 translate into increased amyloid load in WT mice. A recent study comparing (5xFAD mice)

418 and wild type mice [47] showed that cerebrovascular β-amyloid (Aβ) deposition was not

419   affected by 10 weeks of high fat diet in wild type (non-transgenic mice). In line with this, we also

420   evaluated the Aβ levels and the gene expression of proteins involved in Aβ synthesis in

421   prefrontal cortex and hippocampus of wild type and LDLr$^{-/-}$ knockout mice (a model of familiar

422   hypercholesterolemia). According, we did not find changes in Aβ levels or the expression of

423   proteins involved in Aβ processing in either hippocampus or prefrontal cortex of both wild type

424   and LDLr$^{-/-}$ knockout mice [48]. In both studies, memory impairment was not associated with

425   changes in Aβ loading, suggesting that other mechanisms, besides amyloid cascade. Thus, it

426   is unlikely that the observed changes in NTg mice fed a HFCD result from a significant

427   increase in Aβ load in the current study.

428   We also asked if the HFCD intake could exacerbate the behavioral and neurochemical

429   features of the 3xTgAD mouse. These mice develop an age-related and progressive

430   neuropathological phenotype that includes both plaque and tangle pathology in the

431   hippocampus, amygdala and cerebral cortex, with cognitive impairment at 4 and deficits in

432   synaptic plasticity (LTP) at 6 months of age [29,49]. Accordingly, here we observed cognitive

433   impairment in 3 to 4 mo 3xTgAD mouse, expressed as loss of discrimination in both the Y-

434   maze and novel object recognition paradigms. Therefore, we did not verify further decrease

435   in the cognitive function when the 3xTgAD mouse were treated with the HFCD. This fact could

436   be explained due to the qualitative nature of behavior task here performed that evaluates

437   whether the mice learned the task or not. In line with this, previous studies showing that even

438   a long-term high cholesterol (5%) diet intake did not aggravate cognitive deficits in 3xTgAD at

439   7 or 14 mo., despite significantly increasing plasma cholesterol levels [45,46]. The cholesterol

440   enriched diet also increased the locomotion in 3xTgAD mice. In this regard, we have

441   previously shown that cholesterol intake can increase locomotion in LDLr$^{-/-}$ mice, a genetic

442   model of hypercholesterolemia [50]. In general 3xTgAD have been shown to display

443   decreased ambulation and exploratory behavior [51]. In this sense, our data suggests that the

444   increase in plasma cholesterol, induced by a diet high in fat / cholesterol, may alter the

445   locomotion in 3xTgAD mice.

446   Here we observed that the increase in plasma cholesterol levels induced by a HFCD

447   was more pronounced in 3xTgAD mice (around 50%) than in NTg mice (around 10%).

448   Hohsfield *et al.* also observed an increase in plasma cholesterol levels in 3xTgAD mice

449   receiving a diet enriched in cholesterol [45]. This fact suggests deficient management of

450   cholesterol in circulation which may impact vascular metabolic process in 3xTgAD. Previous

451   studies have shown a positive correlation between increased plasma cholesterol levels and

452   β-amyloid load/deposit number in a 2xTgAD mouse model [52–55], suggesting that

453   hypercholesterolemia may somehow aggravate the AD-like pathology.

454   In further exploring events involved in the cognitive impairment related to

455   hypercholesterolemia, we evaluated NMDAr-linked ˙NO production in hippocampal CA1

456   region. Consistent with our previous report, we observed a significant increase in peak ˙NO

457   production in the 3xTgAD mice at this early stage of disease [13]. While the HFCD induced

458   only a tendency for decay in ˙NO concentration dynamics in the NTg mice, it induced a

459   significant decline in the 3xTgAD group. This early-stage increase in ˙NO production at the

460   CA1 synapses in 3xTgAD mice has been proposed to be a compensatory mechanism for loss

461   of synaptic efficacy [56]. We have, however, shown that as the AD-like pathology progresses

462   in the model, a decline in NMDAr-linked ˙NO production is observed (at 12 mo.) despite an

463   increase in total hippocampal nNOS expression [13]. It would appear that in the present study,

464   the HFCD accelerated the age-dependent decline in nitrergic signaling in the CA1 synapse.

465   The decrease in NMDAr-evoked ˙NO production suggests that ˙NO bioavailability may

466   be diverted as a result of the HFCD intake. The mitochondrial complexes are important targets

467   for ˙NO, with implications on respiratory reserve or spare capacity, that is the ability to increase

468   mitochondrial turnover in response to increased energetic demand [57,58]. Age-dependent

469   impairment in oxidative phosphorylation has been reported for 3xTgAD mice in studies using

470   isolated mitochondria [59] as well as hippocampal slices [13]. Here we found no change in

471   hippocampal oxidative phosphorylation at 6 mo. in the 3xTgAD mice. However, the HFCD had

472   a significant effect on tissue oxidative phosphorylation in both NTg and 3xTgAD mice, most

473   importantly on respiratory reserve capacity. Neurons critically depend on mitochondrial

474 function to execute the complex processes of neurotransmission and synaptic plasticity [60]

475 and mitochondrial dysfunction plays a central role in the pathogenesis of neurodegenerative

476 disorders, including AD [61–63]. Increases in neuronal activity impose high ATP demand on

477 neurons and astrocytes, which should be reflected in an increased rate of *in situ* mitochondrial

478 respiration [64]. Failure to meet this increased demand can result in excitotoxicity, one of the

479 key mechanisms of neurodegeneration [65,66]. Mitochondrial respiratory spare capacity

480 allows tissues to adequately respond to situations of increased energy demand [67], which we

481 see here is compromised as a result of fat/cholesterol overconsumption. Depletion of the spare

482 capacity has been related to a range of pathologies affecting high energy requiring tissues

483 such as the brain [67–69]. The mitochondrial dysfunction seen here may be due to a change

484 in the phospholipid composition of the mitochondrial membranes [70], which have been

485 associated with synaptic mitochondrial dysfunction [71].

486 One critical issue that remains poorly understood is how systemic cholesterol can impact

487 neuronal function, considering that brain cholesterol homeostasis is segregated from

488 peripheral circulation and that CNS and plasma cholesterol/lipoprotein compartments are

489 separated by the BBB in healthy subjects [72]. One hypothesis is that the cellular components

490 of blood brain barrier (BBB) can be affected by high circulating cholesterol levels or even by

491 the high fat intake, and/or by β-amyloid load/deposit. Herein AQP-4 and tomato lectin

492 immunofluorescence were used as putative biomarkers of changes in the BBB. AQP-4 is an

493 integral membrane protein at the feet of the astrocytes that serves as water channels in BBB

494 [73]. We observed an intense effect of genotype in increasing the AQP-4 immunostaining in

495 the hippocampal CA1 region of 3xTgAD mice which were intensified by HFCD. The same

496 pattern was visualized for tomato lectin staining, a protein obtained from *Lycopersicum*

497 *esculentum* with specific affinity for poly-N-acetyl lactosamine sugar residues, which are found

498 on the plasma membrane of endothelial cells and in the cytoplasm of microglia [74]. These

499 changes suggest structural defects in the astrocytic endfeet associated with the

500 microvasculature, with expected consequences in terms of BBB functionally. Our data indicate

501 that the amyloidogenic pathway associated with a persistent exposure of endothelial cells to

502   increased cholesterol levels impacts the key components of neurovascular unit. Studies in

503   rabbits have shown that, alongside increased accumulation of hippocampal Aβ, a cholesterol-

504   enriched diet can increase BBB permeability [75,76], which has also been verified in the

505   hippocampus of rats [77].

506

507   **Conclusions**

508   The results of the present study suggest that learning and memory processes,

509   particularly those that rely on the integrity of the hippocampus, are susceptible to disruption

510   by diets containing high levels of fat and cholesterol. Our data indicates a short-term HCFD

511   capable of increasing circulating cholesterol levels in NTg mice by a non-significant value of

512   10%, produces an AD-like phenotype in mice, inducing compromised learning and memory

513   and a decrease in NMDAr-linked ˙NO production. Otherwise, 3xTgAD were more susceptible

514   to increase the plasma cholesterol load impacting in hippocampal markers of NVU.

515   Furthermore, this fat/cholesterol enriched diet induces a compromise in oxidative

516   phosphorylation in both NTg and 3xTgAD hippocampus, recapitulating important

517   mitochondrial/metabolic perturbations observed in AD patients but poorly represented in the

518   transgenic mouse model of AD. Changes in the organization of NVU components may

519   putatively connect the bioenergetic crises and cognitive impairment, a hypothesis which

520   renders further structural and functional studies to be better corroborated. Considering that in

521   the sporadic forms of AD in humans, factors associated with cardiovascular disease such as

522   hypercholesterolemia are paired with age as important risk factors for AD, one may propose

523   that such models as the one used here encompassing a high fat and cholesterol diets may

524   better recapitulate the pathophysiology of AD.

525

539

540 **Conflict of Interest/Disclosure Statement**: The authors have no conflict of interest to report.

Figure Captions:

542
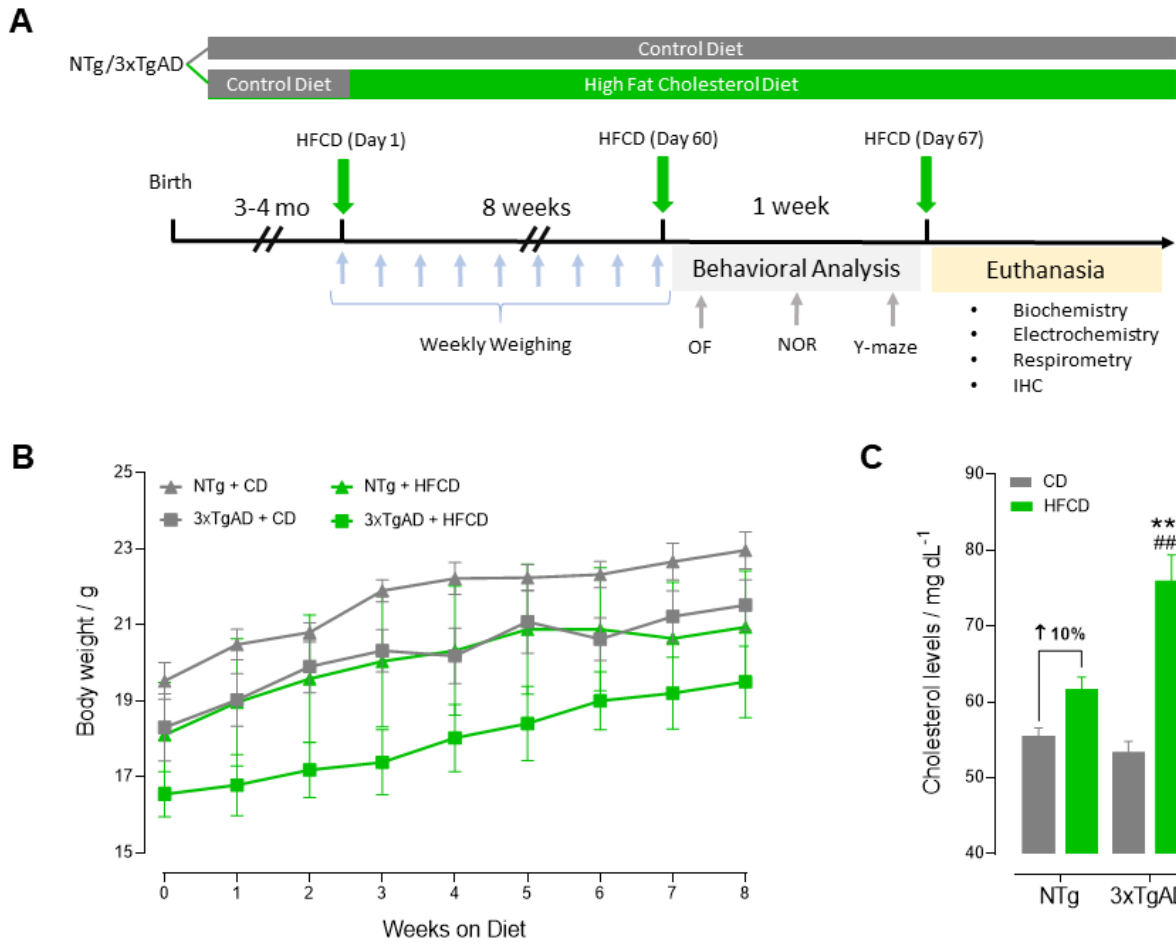
Figure 1. Experimental design, body weight and plasma cholesterol levels. A - Timeline

of experimental design used in the present study; B - body weight profile for all animal groups

throughout the 8-week treatment; C - plasma cholesterol levels determined at the end of the

8-week treatment. Data are expressed as mean ± SEM from six to eight animals per group,

with [###]$p < 0.001$ when determining the effect of diet for the same genotype and [***]$p<0.001$

when determining the effect of genotype (2-way ANOVA followed by Bonferroni *post hoc* test).

549

550

551

552

553

554
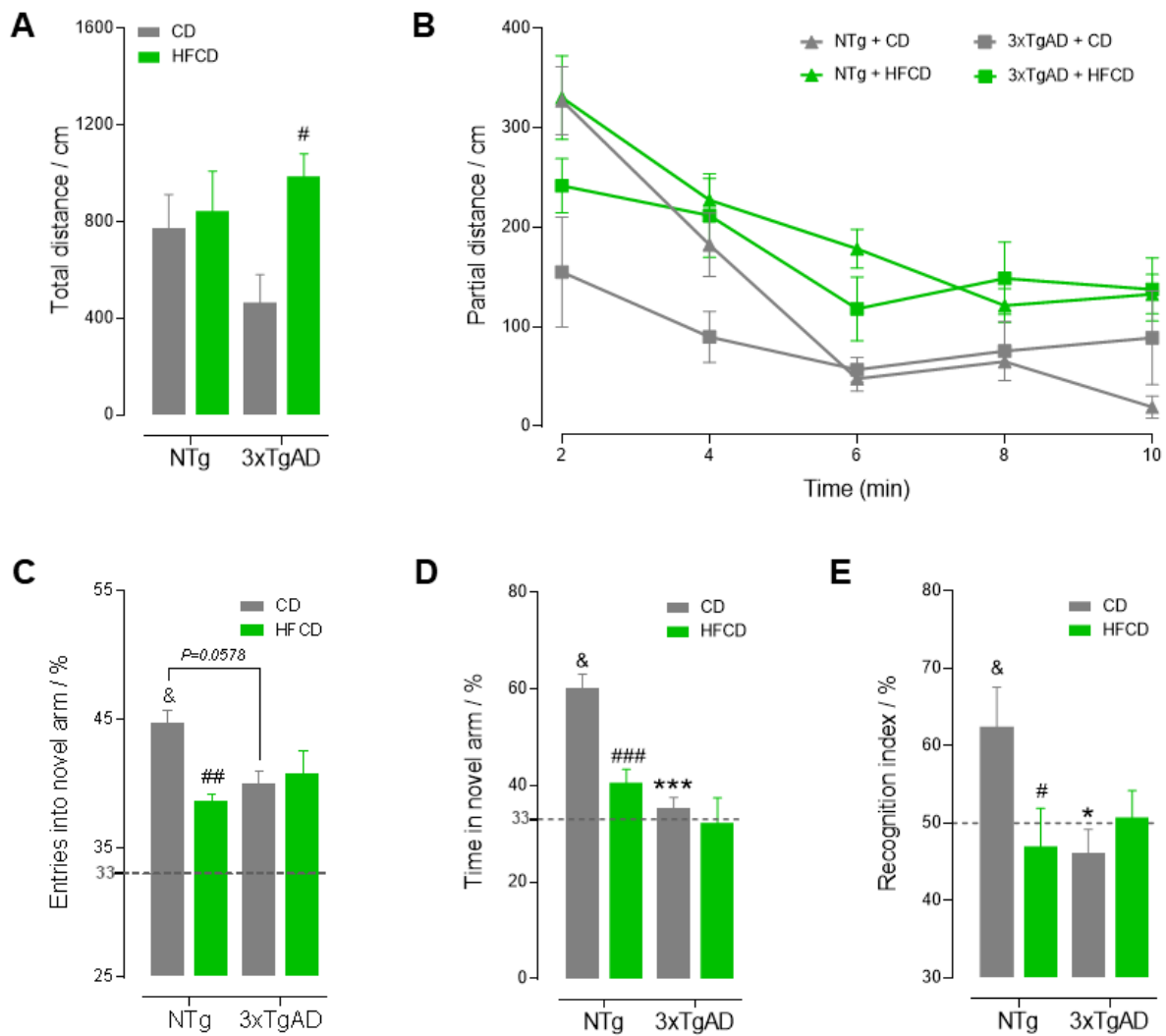
Figure 2. High-fat and cholesterol diet induces significant changes in locomotor activity and cognitive performance in NTg mice. A – Total distance travelled due to spontaneous locomotor activity in an open field apparatus during the full 10 min period and; B – Profile of locomotor activity, evaluated as partial distance for each 2-min bin; C - Relative percentage of entries into each arm in a Y-maze spontaneous alternation test and D - Percentage of time spent in each arm; E - Recognition index for evaluation of recognition memory using a 2-object novel object recognition test (NOR). Data are expressed as mean ± SEM from six to eight animals per group. #$p<0.05$, ##$p<0.01$ and ###$p<0.001$, when determining the effect of diet for the same genotype, *$p<0.05$, ***$p < 0.001$ when determining the effect of genotype (2-way ANOVA followed by Bonferroni post hoc test). & $p<0.05$ compared to the hypothetical value (random investigation) of 33% or 50% for the modified Y maze and NOR test, respectively.

567
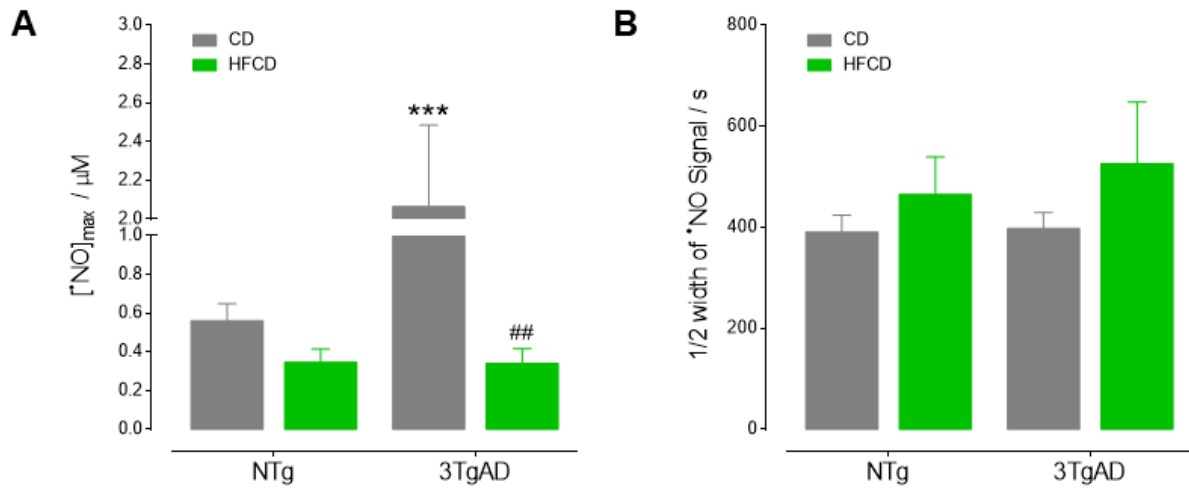
Figure 3. Effect of a high fat/cholesterol diet on hippocampal ·NO concentration dynamics in NTg and 3xTg-AD mice. A – Average maximal change in ·NO concentration achieved following transient activation of NMDAr (2 min, 100 µM), measured in the CA1 subregion; B – Average 1/2 width of ·NO signal. Data are expressed as mean ± SEM from five to six animals per group. [##]$p< 0.01$, when determining the effect of diet for the same genotype and [***] $p< 0.001$, when determining the effect of genotype (2-way ANOVA followed by Bonferroni post hoc test).
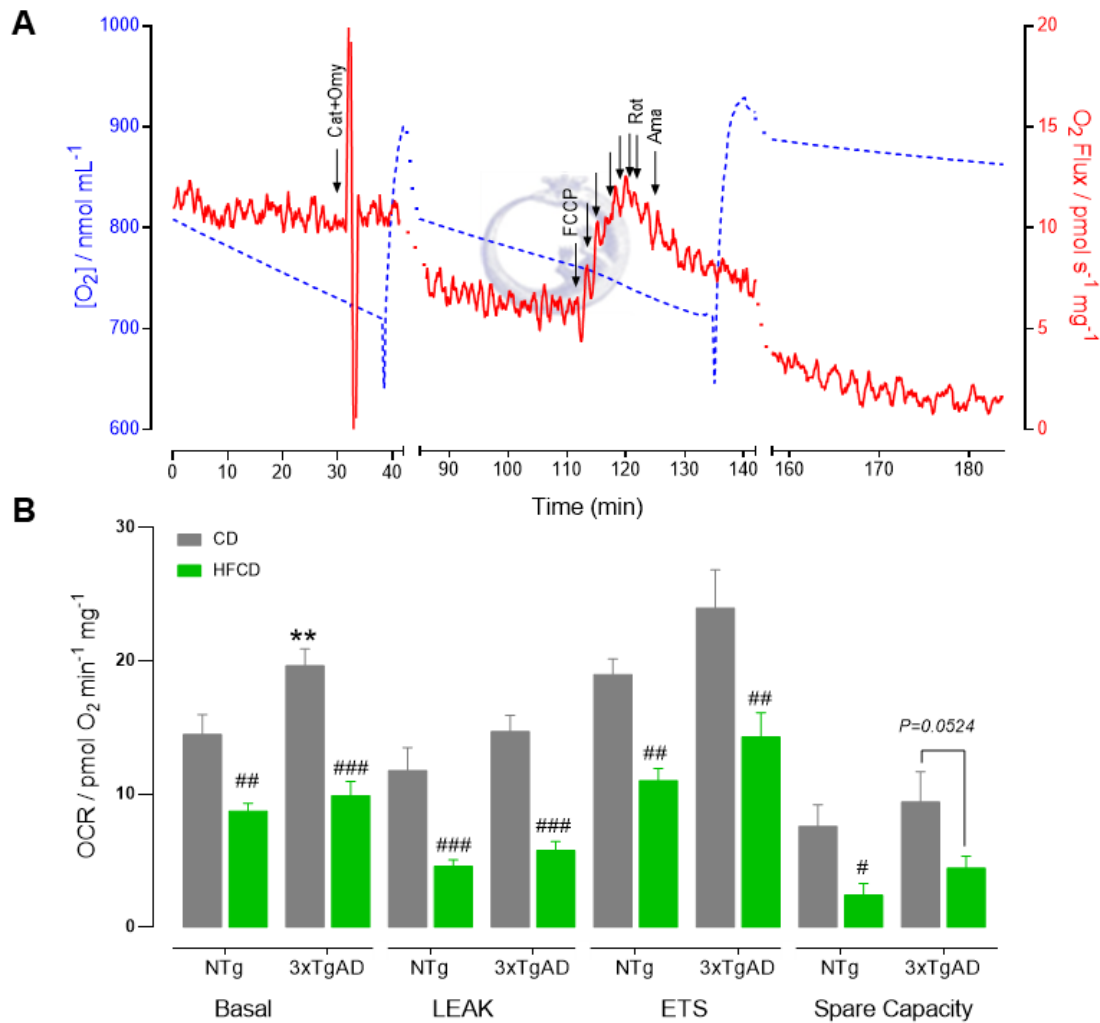
Figure 4. Effect of a high fat/cholesterol diet on hippocampal mitochondrial oxygen consumption in NTg and 3xTg-AD mice. A - Representative oxygraphy trace of oxygen concentration (dashed blue line) and oxygen flux corrected for tissue wet weight (solid red line) of a SUIT protocol performed in intact hippocampal slices using high-resolution respirometry; B – Average O_2 consumption rates (OCR) measured at 4 points of the evaluation, namely Basal OCR (O_2 consumed due to oxidation of exogenous substrates glucose and pyruvate), LEAK (OCR not dependent on ATP production), ETS (maximal respiratory rate resulting from uncoupled mitochondrial respiration) and spare respiratory capacity. Cat: Carboxyatractyloside, Omy: oligomycin, FCCP: Carbonyl cyanide 4-(trifluoromethoxy) phenylhydrazone, Rot: rotenone, Ama: antimycin-A. Data are expressed as mean ± SEM of the mean of six to eight animals per group. *##p< 0.01 and ##p< 0.001* when

determining the effect of diet for the same genotype; **$p< 0.01$, when determining the effect of genotype (2-way ANOVA followed by Bonferroni post hoc test).
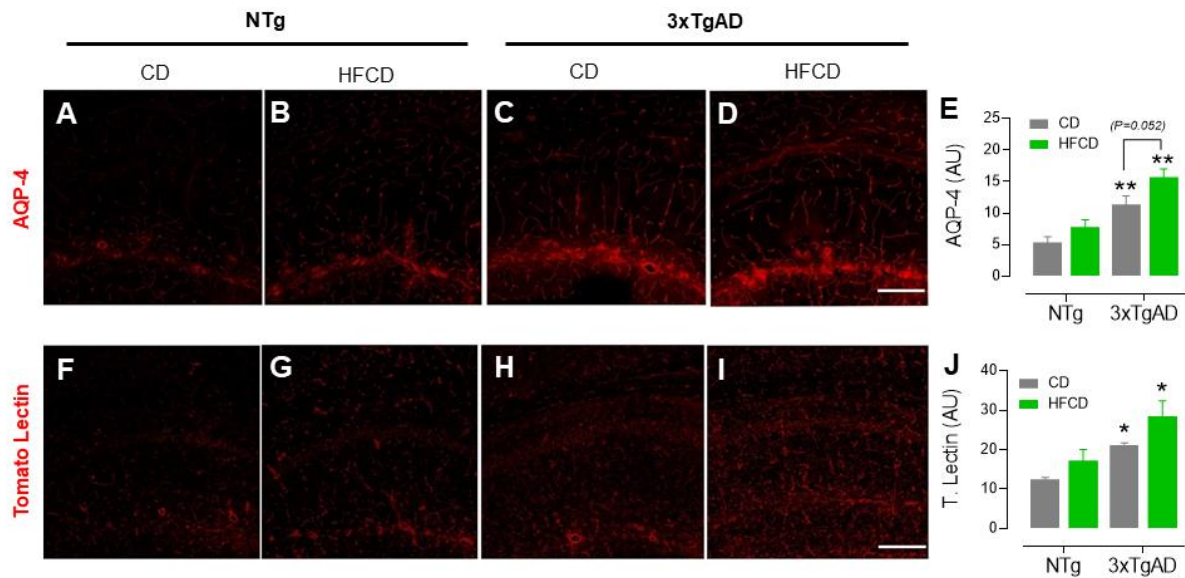
Figure 5. Effect of a high fat/cholesterol diet on cellular components of the neurovascular unit in CA1 subregion of the hippocampus of NTg and 3xTg-AD mice. A-D - Representative images of AQP-4 immunostain in the CA1 subregion of the hippocampus; E – Quantification of AQP-4 immunofluorescence; F-I – Representative micrographs of Tomato Lectin immunostrain in the CA1 subregion of the hippocampus; J – Quantification of Tomato Lectin immunofluorescence. Scale bars, 100 µm. *$P < 0.05$ and **$P < 0.01$ when determining the effect of genotype for the same diet (2-way ANOVA followed by Bonferroni).

References

[1]   Imtiaz B, Tolppanen A-M, Kivipelto M, Soininen H (2014) Future directions in Alzheimer's disease from risk factors to prevention. *Biochem Pharmacol* **88**, 661–670.

[2]   Kivipelto M, Ngandu T, Fratiglioni L, Viitanen M, Kareholt I, Winblad B, Helkala EL, Tuomilehto J, Soininen H, Nissinen A (2005) Obesity and vascular risk factors at midlife and the risk of dementia and Alzheimer disease. *Arch Neurol* **62**, 1556–1560.

[3]   Solomon A, Kivipelto M, Wolozin B, Zhou J, Whitmer RA (2009) Midlife serum cholesterol and increased risk of Alzheimer's and vascular dementia three decades later. *Dement Geriatr Cogn Disord* **28**, 75–80.

[4]   Kivipelto M, Laakso MP, Tuomilehto J, Nissinen A, Soininen H (2002) Hypertension and hypercholesterolaemia as risk factors for Alzheimer's disease: potential for pharmacological intervention. *CNS Drugs* **16**, 435–44.

[5]   Casserly I, Topol E (2004) Convergence of atherosclerosis and Alzheimer's disease: inflammation, cholesterol, and misfolded proteins. *Lancet (London, England)* **363**, 1139–46.

[6]   Vagelatos NT, Eslick GD (2013) Type 2 diabetes as a risk factor for Alzheimer's disease: The confounders, interactions, and neuropathology associated with this relationship. *Epidemiol Rev* **35**, 152–160.

[7]   Puglielli L, Tanzi RE, Kovacs DM (2003) Alzheimer's disease: the cholesterol connection. *Nat Neurosci* **6**, 345–51.

[8]   Corder E, Saunders A, Strittmatter W, Schmechel D, Gaskell P, Small G, Roses A, Haines J, Pericak-Vance M (1993) Gene dose of apolipoprotein E type 4 allele and the risk of Alzheimer's disease in late onset families. *Science (80-)* **261**, 921–923.

[9]   Bertram L, Tanzi RE (2008) Thirty years of Alzheimer's disease genetics: the implications of systematic meta-analyses. *Nat Rev Neurosci* **9**, 768–778.

[10]   Grammas P, Martinez J, Miller B (2011) Cerebral microvascular endothelium and the pathogenesis of neurodegenerative diseases. *Expert Rev Mol Med* **13**, e19.

[11]   De la Torre JC, Mussivand T (1993) Can disturbed brain microcirculation cause

632   Alzheimer's disease? *Neurol Res* **15**, 146–153.

633   [12]   Humpel C (2011) Chronic mild cerebrovascular dysfunction as a cause for Alzheimer's

634   disease? *Exp Gerontol* **46**, 225–232.

635   [13]   Dias C, Lourenço CF, Ferreiro E, Barbosa RM, Laranjinha J, Ledo A (2016) Age-

636   dependent changes in the glutamate-nitric oxide pathway in the hippocampus of the

637   triple transgenic model of Alzheimer's disease: implications for neurometabolic

638   regulation. *Neurobiol Aging* **46**, 84–95.

639   [14]   Yin F, Sancheti H, Patil I, Cadenas E (2016) Energy metabolism and inflammation in

640   brain aging and Alzheimer's disease. *Free Radic Biol Med* **100**, 108–122.

641   [15]   Schmitt K, Grimm A, Kazmierczak A, Strosznajder JB, Götz J, Eckert A (2012) Insights

642   into Mitochondrial Dysfunction: Aging, Amyloid-β, and Tau–A Deleterious Trio. *Antioxid*

643   *Redox Signal* **16**, 1456–1466.

644   [16]   Keller JN, Schmitt F a, Scheff SW, Ding Q, Chen Q, Butterfield D a, Markesbery WR

645   (2005) Evidence of increased oxidative damage in subjects with mild cognitive

646   impairment. *Neurology* **64**, 1152–6.

647   [17]   Migliore L, Fontana I, Trippi F, Colognato R, Coppedè F, Tognoni G, Nucciarone B,

648   Siciliano G (2005) Oxidative DNA damage in peripheral leukocytes of mild cognitive

649   impairment and AD patients. *Neurobiol Aging* **26**, 567–573.

650   [18]   Mosconi L (2005) Brain glucose metabolism in the early and specific diagnosis of

651   Alzheimer's disease: FDG-PET studies in MCI and AD. *Eur J Nucl Med Mol Imaging*

652   **32**, 486–510.

653   [19]   Mosconi L, Pupi A, De Leon MJ (2008) Brain glucose hypometabolism and oxidative

654   stress in preclinical Alzheimer's disease. *Ann N Y Acad Sci* **1147**, 180–195.

655   [20]   Mosconi L, Mistur R, Switalski R, Tsui WH, Glodzik L, Li Y, Pirraglia E, De Santi S,

656   Reisberg B, Wisniewski T, De Leon MJ (2009) FDG-PET changes in brain glucose

657   metabolism from normal cognition to pathologically verified Alzheimer's disease. *Eur J*

658   *Nucl Med Mol Imaging* **36**, 811–822.

659   [21]   Asiimwe N, Yeo SG, Kim M-S, Jung J, Jeong NY (2016) Nitric Oxide: Exploring the

660   Contextual Link with Alzheimer's Disease. *Oxid Med Cell Longev* **2016**, 1–10.

661 [22] Garthwaite J (2008) Concepts of neural nitric oxide-mediated transmission. *Eur J*

662   *Neurosci* **27**, 2783–802.

663 [23] Ledo A, Barbosa RM, Gerhardt GA, Cadenas E, Laranjinha J (2005) Concentration

664   dynamics of nitric oxide in rat hippocampal subregions evoked by stimulation of the

665   NMDA glutamate receptor. *Proc Natl Acad Sci* **102**, 17483–17488.

666 [24] Prast H, Philippu A (2001) Nitric oxide as modulator of neuronal function. *Prog*

667   *Neurobiol* **64**, 51–68.

668 [25] Edwards TM, Rickard NS (2007) New perspectives on the mechanisms through which

669   nitric oxide may affect learning and memory processes. *Neurosci Biobehav Rev* **31**,

670   413–425.

671 [26] Ledo A, Lourenço CF, Cadenas E, Barbosa RM, Laranjinha J (2021) The bioactivity of

672   neuronal-derived nitric oxide in aging and neurodegeneration: Switching signaling to

673   degeneration. *Free Radic Biol Med* **162**, 500–513.

674 [27] Lourenço CF, Ledo A, Barbosa RM, Laranjinha J (2017) Neurovascular-neuroenergetic

675   coupling axis in the brain: master regulation by nitric oxide and consequences in aging

676   and neurodegeneration. *Free Radic Biol Med* **108**, 668–682.

677 [28] Moodley KK, Chan D (2014) The hippocampus in neurodegenerative disease. *Front*

678   *Neurol Neurosci* **34**, 95–108.

679 [29] Oddo S, Caccamo A, Shepherd JD, Murphy MP, Golde TE, Kayed R, Metherate R,

680   Mattson MP, Akbari Y, LaFerla FM (2003) Triple-transgenic model of Alzheimer's

681   disease with plaques and tangles: intracellular Abeta and synaptic dysfunction. *Neuron*

682   **39**, 409–21.

683 [30] Leger M, Quiedeville A, Bouet V, Haelewyn B, Boulouard M, Schumann-Bard P, Freret

684   T (2013) Object recognition test in mice. *Nat Protoc* **8**, 2531–2537.

685 [31] Soares E, Prediger RD, Nunes S, Castro AA, Viana SD, Lemos C, De Souza CM,

686   Agostinho P, Cunha RA, Carvalho E, Fontes Ribeiro CA, Reis F, Pereira FC (2013)

687   Spatial memory impairments in a prediabetic rat model. *Neuroscience* **250**, 565–577.

688 [32] Ferreira NR, Ledo A, Frade JG, Gerhardt GA, Laranjinha J, Barbosa RM (2005)

689 Electrochemical measurement of endogenously produced nitric oxide in brain slices

690 using Nafion/o-phenylenediamine modified carbon fiber microelectrodes. *Anal Chim*

691 *Acta* **535**, 1–7.

692 [33] Ledo A, Barbosa RM, Laranjinha J (2012) Modulation of cellular respiration by

693 endogenously produced nitric oxide in rat hippocampal slices. *Methods Mol Biol* **810**,

694 73–88.

695 [34] Dias C, Lourenço CF, Barbosa RM, Laranjinha J, Ledo A (2018) Analysis of respiratory

696 capacity in brain tissue preparations: high-resolution respirometry for intact

697 hippocampal slices. *Anal Biochem* **551**, 43–50.

698 [35] Pesta D, Gnaiger E (2012) High-resolution respirometry: OXPHOS protocols for human

699 cells and permeabilized fibers from small biopsies of human muscle. *Methods Mol Biol*

700 **810**, 25–58.

701 [36] Clark JK, Furgerson M, Crystal JD, Fechheimer M, Furukawa R, Wagner JJ (2015)

702 Alterations in synaptic plasticity coincide with deficits in spatial working memory in

703 presymptomatic 3xTg-AD mice. *Neurobiol Learn Mem* **125**, 152–162.

704 [37] Knight EM, Martins IVA, Gümüsgöz S, Allan SM, Lawrence CB (2014) High-fat diet-

705 induced memory impairment in triple-transgenic Alzheimer's disease (3xTgAD) mice

706 is independent of changes in amyloid and tau pathology. *Neurobiol Aging* **35**, 1821–

707 1832.

708 [38] Anstey KJ, Ashby-Mitchell K, Peters R (2017) Updating the evidence on the association

709 between serum cholesterol and risk of late-life dementia: Review and meta-analysis. *J*

710 *Alzheimer's Dis* **56**, 215–228.

711 [39] Davidson TL, Hargrave SL, Swithers SE, Sample CH, Fu X, Kinzig KP, Zheng W (2013)

712 Inter-relationships among diet, obesity and hippocampal-dependent cognitive function.

713 *Neuroscience* **253**, 110–122.

714 [40] Moreira ELG, de Oliveira J, Engel DFFF, Walz R, De Bem AF, Farina M, Prediger RDS

715 (2014) Hypercholesterolemia induces short-term spatial memory impairments in mice:

716   Up-regulation of acetylcholinesterase activity as an early and causal event? *J Neural*

717   *Transm* **121**, 415–426.

718   [41] Elder GA, Ragnauth A, Dorr N, Franciosi S, Schmeidler J, Haroutunian V, Buxbaum JD

719   (2008) Increased locomotor activity in mice lacking the low-density lipoprotein receptor.

720   *Behav Brain Res* **191**, 256–265.

721   [42] Sanderson DJ, Bannerman DM (2012) The role of habituation in hippocampus-

722   dependent spatial working memory tasks: Evidence from GluA1 AMPA receptor subunit

723   knockout mice. *Hippocampus* **22**, 981–994.

724   [43] de Oliveira J, Hort MA, Moreira ELG, Glaser V, Ribeiro-do-Valle RM, Prediger RD,

725   Farina M, Latini A, de Bem AF (2011) Positive correlation between elevated plasma

726   cholesterol levels and cognitive impairments in LDL receptor knockout mice: relevance

727   of cortico-cerebral mitochondrial dysfunction and oxidative stress. *Neuroscience* **197**,

728   99–106.

729   [44] Ullrich C, Pirchl M, Humpel C (2010) Hypercholesterolemia in rats impairs the

730   cholinergic system and leads to memory deficits. *Mol Cell Neurosci* **45**, 408–417.

731   [45] Hohsfield LA, Daschil N, Orädd G, Strömberg I, Humpel C (2014) Vascular pathology

732   of 20-month-old hypercholesterolemia mice in comparison to triple-transgenic and

733   APPSwDI Alzheimer's disease mouse models. *Mol Cell Neurosci* **63**, 83–95.

734   [46] Löffler T, Schweinzer C, Flunkert S, Sántha M, Windisch M, Steyrer E, Hutter-Paier B

735   (2016) Brain cortical cholesterol metabolism is highly affected by human APP

736   overexpression in mice. *Mol Cell Neurosci* **74**, 34–41.

737   [47] Lin B, Hasegawa Y, Takane K, Koibuchi N, Cao C, Kim-Mitsuyama S (2016) High-Fat-

738   Diet Intake Enhances Cerebral Amyloid Angiopathy and Cognitive Impairment in a

739   Mouse Model of Alzheimer's Disease, Independently of Metabolic Disorders. *J Am*

740   *Heart Assoc* **5**, e003154.

741   [48] De Oliveira J, Engel DF, De Paula GC, Melo HM, Lopes SC, Ribeiro CT, Delanogare

742   E, Moreira JCF, Gelain DP, Prediger RD, Gabilan NH, Moreira ELG, Ferreira ST, De

743   Bem AF (2020) LDL Receptor Deficiency Does not Alter Brain Amyloid-β Levels but

744   Causes an Exacerbation of Apoptosis. *J Alzheimer's Dis* **73**, 585–596.

745 [49] Billings LM, Oddo S, Green KN, McGaugh JL, LaFerla FM (2005) Intraneuronal Abeta

746   causes the onset of early Alzheimer's disease-related cognitive deficits in transgenic

747   mice. *Neuron* **45**, 675–88.

748 [50] De Oliveira J, Engel DF, De Paula GC, Dos Santos DB, Lopes JB, Farina M, Moreira

749   ELG, De Bem AF (2020) High Cholesterol Diet Exacerbates Blood-Brain Barrier

750   Disruption in LDLr-/- Mice: Impact on Cognitive Function. *J Alzheimer's Dis* **78**, 97–115.

751 [51] Sterniczuk R, Antle MC, Laferla FM, Dyck RH (2010) Characterization of the 3xTg-AD

752   mouse model of Alzheimer's disease: part 2. Behavioral and cognitive changes. *Brain*

753   *Res* **1348**, 149–55.

754 [52] Sah SK, Lee C, Jang J-H, Park GH (2017) Effect of high-fat diet on cognitive impairment

755   in triple-transgenic mice model of Alzheimer's disease. *Biochem Biophys Res Commun*

756   **493**, 731–736.

757 [53] Ettcheto M, Petrov D, Pedrós I, Alva N, Carbonell T, Beas-Zarate C, Pallas M, Auladell

758   C, Folch J, Camins A (2016) Evaluation of Neuropathological Effects of a High-Fat Diet

759   in a Presymptomatic Alzheimer's Disease Stage in APP/PS1 Mice. *J Alzheimer's Dis*

760   **54**, 233–251.

761 [54] Knight EM, Verkhratsky A, Luckman SM, Allan SM, Lawrence CB (2012)

762   Hypermetabolism in a triple-transgenic mouse model of Alzheimer's disease. *Neurobiol*

763   *Aging* **33**, 187–193.

764 [55] Refolo LM, Pappolla M a, Malester B, LaFrancois J, Bryant-Thomas T, Wang R, Tint

765   GS, Sambamurti K, Duff K (2000) Hypercholesterolemia accelerates the Alzheimer's

766   amyloid pathology in a transgenic mouse model. *Neurobiol Dis* **7**, 321–331.

767 [56] Chakroborty S, Kim J, Schneider C, West AR, Stutzmann GE (2015) Nitric oxide

768   signaling is recruited as a compensatory mechanism for sustaining synaptic plasticity

769   in Alzheimer's disease mice. *J Neurosci* **35**, 6893–902.

770 [57] Dranka BP, Hill BG, Darley-Usmar VM (2010) Mitochondrial reserve capacity in

771   endothelial cells: The impact of nitric oxide and reactive oxygen species. *Free Radic*

772   *Biol Med* **48**, 905–914.

773   [58]   Nicholls DG (2009) Spare respiratory capacity, oxidative stress and excitotoxicity.

774   *Biochem Soc Trans* **37**, 1385–1388.

775   [59]   Yao J, Irwin RW, Zhao L, Nilsen J, Hamilton RT, Brinton RD (2009) Mitochondrial

776   bioenergetic deficit precedes Alzheimer's pathology in female mouse model of

777   Alzheimer's disease. *Proc Natl Acad Sci U S A* **106**, 14670–14675.

778   [60]   Kann O, Kovács R, Kovacs R (2007) Mitochondria and neuronal activity. *Am J Physiol*

779   *Cell Physiol* **292**, C641-657.

780   [61]   Piaceri I, Rinnoci V, Bagnoli S, Failli Y, Sorbi S (2012) Mitochondria and Alzheimer's

781   disease. *J Neurol Sci* **322**, 31–34.

782   [62]   Gu XM, Huang HC, Jiang ZF (2012) Mitochondrial dysfunction and cellular metabolic

783   deficiency in Alzheimer's disease. *Neurosci Bull* **28**, 631–640.

784   [63]   Johri A, Beal MF (2012) Mitochondrial dysfunction in neurodegenerative diseases. *J*

785   *Pharmacol Exp Ther* **342**, 619–30.

786   [64]   Jekabsons MB, Nicholls DG (2004) In Situ respiration and bioenergetic status of

787   mitochondria in primary cerebellar granule neuronal cultures exposed continuously to

788   glutamate. *J Biol Chem* **279**, 32989–33000.

789   [65]   Butterfield DA, Pocernich CB (2003) The glutamatergic system and Alzheimer's

790   disease: Therapeutic implications. *CNS Drugs* **17**, 641–652.

791   [66]   Cowburn RF, Hardy JA, Roberts PJ (1990) Glutamatergic neurotransmission in

792   Alzheimer's disease. *BiochemSocTrans* **18**, 390–392.

793   [67]   Yadava N, Nicholls DG (2007) Spare respiratory capacity rather than oxidative stress

794   regulates glutamate excitotoxicity after partial respiratory inhibition of mitochondrial

795   complex I with rotenone. *J Neurosci* **27**, 7310–7317.

796   [68]   Nicholls DG (2008) Oxidative stress and energy crises in neuronal dysfunction. *Ann N*

797   *Y Acad Sci* **1147**, 53–60.

798   [69]   Desler C, Hansen TL, Frederiksen JB, Marcker ML, Singh KK, Juel Rasmussen L

799   (2012) Is there a link between mitochondrial reserve respiratory capacity and aging? *J*

800   *Aging Res* **2012**,.

801   [70]   Nam KN, Mounier A, Wolfe CM, Fitz NF, Carter AY, Castranio EL, Kamboh HI, Reeves

802   VL, Wang J, Han X, Schug J, Lefterov I, Koldamova R (2017) Effect of high fat diet on

803   phenotype, brain transcriptome and lipidome in Alzheimer's model mice. *Sci Rep* **7**,

804   4307.

805   [71]   Monteiro-Cardoso VF, Oliveira MM, Melo T, Domingues MRM, Moreira PI, Ferreiro E,

806   Peixoto F, Videira RA (2014) Cardiolipin Profile Changes are Associated to the Early

807   Synaptic Mitochondrial Dysfunction in Alzheimer's Disease. *J Alzheimer's Dis* **43**,

808   1375–1392.

809   [72]   Dietschy JM, Turley SD (2001) Cholesterol metabolism in the brain. *Curr Opin Lipidol*

810   **12**, 105–112.

811   [73]   Isasi E, Barbeito L, Olivera-Bravo S (2014) Increased blood-brain barrier permeability

812   and alterations in perivascular astrocytes and pericytes induced by intracisternal

813   glutaric acid. *Fluids Barriers CNS* **11**, 1–12.

814   [74]   Acarin L, Vela JM, González B, Castellano B (1994) Demonstration of poly-N-acetyl

815   lactosamine residues in ameboid and ramified microglial cells in rat brain by tomato

816   lectin binding. *J Histochem Cytochem* **42**, 1033–1041.

817   [75]   Sparks DL (2008) The Early and Ongoing Experience with the Cholesterol-Fed Rabbit

818   as a Model of Alzheimer's Disease: The Old, the New and the Pilot. *J Alzheimer's Dis*

819   **15**, 641–656.

820   [76]   Chen X, Ghribi O, Geiger JD (2008) Rabbits fed cholesterol-enriched diets exhibit

821   pathological features of inclusion body myositis. *Am J Physiol - Regul Integr Comp*

822   *Physiol* **294**,.

823   [77]   Kanoski SE, Zhang Y, Zheng W, Davidson TL (2010) The effects of a high-energy diet

824   on hippocampal function and blood-brain barrier integrity in the rat. *J Alzheimer's Dis*.

825